

MECHANICAL DESIGN OF SECONDARY SOURCE SLITS FOR HARD X-RAY BEAMLINES AT TAIWAN PHOTON SOURCE

H. Y. Yan[†], C. H. Chang, D. J. Wang, C. Y. Chen, J. M. Lin, C. Y. Huang, D. G. Liu, S. H. Chang
National Synchrotron Radiation Research Center, Hsinchu, Taiwan

Abstract

The secondary source slits have been developed for specific hard X-ray beamlines at Taiwan Photon Source. Especially for Coherent X-ray Scattering and X-ray Nanoprobe beamlines, severe specifications of the slits are more necessary to define proper beam sizes in horizontal and vertical directions at sample. The opening size of each pair of slits assembled orthogonally is usually needed to range within several microns, so the UHV-compatible piezo-driven stages with closed-loop system were adopted for the purposes of fine adjustment, precise positional accuracy and repeatability. To reduce X-ray scattering effect, the rectangular single-crystal film was bonded on the edge of the slit blade. The machined rotary weak-link structure and piezo-driven actuators were used to slightly adjust parallelism of each pair of the blades with the method of single-slit diffraction. To enhance structural and thermal stability, the granite plinths with specified shape were designed and the precise temperature controlling system will be set up recently. The overall design, mechanical specifications and procedure of testing for secondary source slits will be introduced in this paper.

INTRODUCTION

As small beam size is more required in hard X-ray beamlines at accelerators of synchrotron radiation around the world, the specifications of slits system become more critical. For example, the beam size between 1 - 10 μm both in horizontal and vertical directions at sample was design for the Coherent X-ray Scattering beamline at Taiwan Photon Source (TPS). The quality of beam spot with small size is influenced by unstable situation very easily, so mechanical stability of slits system needs to be considered comprehensively. For these reasons, the necessity of designing a new type of mono beam secondary source slits was taken into account. Recently we have developed a new type of stable slits system with severe specifications, such as the smallest opening size and parallelism between two blades on each pair of slits. The following sections will introduce design of secondary source slits, testing procedure and result, and precise temperature controlling system respectively.

DESIGN OF SECONDARY SOURCE SLITS

To achieve the expected performance, some commercial components used widely were adopted in the mono beam secondary source slits for their mature developing experience. And the specific design for accurate adjustment and mechanical stability were completed. Fig. 1 and Fig. 2 show the schematic 3-D drawing and on-site view of secondary source slits installed in the Coherent X-ray Scattering beamline and located at 40.52 m from the center of

two Insertion Devices respectively. Considering the optical design, the slits system is uncooled type because of locating after the Double Crystal Monochromator (DCM).

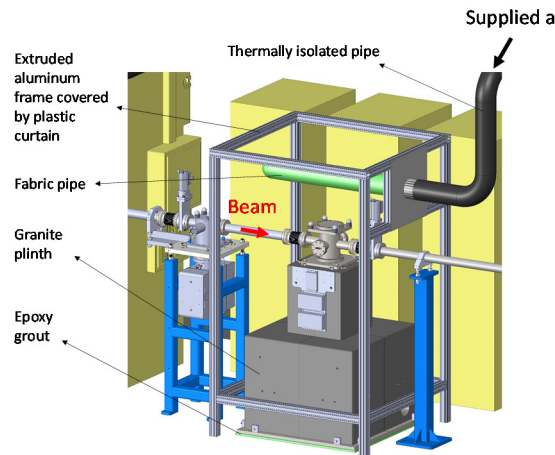


Figure 1: Schematic 3-D drawing of secondary source slits.



Figure 2: On-site view of secondary source slits installed in the Coherent X-ray Scattering beamline at TPS.

Specifications

Fig. 3 shows a 3-D model of main mechanism for secondary source slits. Gap between blades of each slit is maintained to produce zero beam. Two sets of piezo-driven actuator were adopted for their accurate size for each step and compatibility of ultra-high vacuum (UHV). Piezo stages with closed-looped system function for controlling opening size of each pair of slits, and their positional accuracy and repeatability are both less than 100 nm. Picomotors are used to adjust parallelism between blades of each

slit, and size for each step is less than 30 nm. Tungsten carbide is taken as material of blades. Specifically, rectangular single-crystal film is bonded on the edge of the slit blade to reduce X-ray scattering effect. The overall specifications of secondary source slits are specified in Table 1.

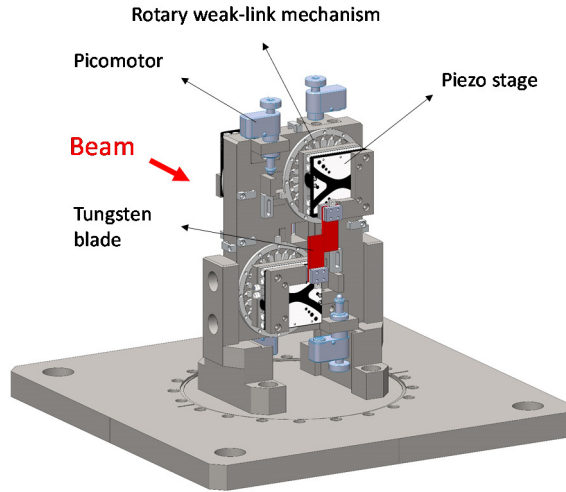


Figure 3: A 3-D model of main mechanism for secondary source slits.

Table 1: The Overall Specifications of Secondary Source Slits

Item	Specification
Vacuum	$\leq 10^{-9}$ mbar
Helium leak rate	$\leq 5 \times 10^{-10}$ mbar·l/s
Material	Tungsten carbide (Type WF20: 86.4% WC, 11.5% Co, 2.1% Others) GaAs single crystal
Maximum opening size	13 mm (H) \times 13 mm (V)
Position resolution	≤ 0.006 μ m
Position repeatability	≤ 0.018 μ m
Positional accuracy	≤ 0.2 μ m
Parallelism between blades	≤ 1 μ m
Range of rotary adjustment	± 0.21 degree

Design of Mechanical Stability

The rotary weak-link mechanism [1] was developed for slightly rotary movement with high stiffness and stability, so it is very suitable for adjustment of parallelism of two blades of each slit. The rotary weak-link structure is shaped with complex axisymmetric geometry and has 3 mm of thickness. Except for wire electrical discharge machining (WEDM), ordinary machining methods are not able to realize the design.

SOLIDWORKS Simulation software was used as a tool of finite-element analysis to verify the statistical mechanics of rotary weak-link mechanism. The boundary conditions

consist of the centric constraint and torque forced by picomotor. SUS630 H900 stainless steel was chosen as material of rotary weak-link mechanism for its high yielding stress. Result of finite-element analysis is shown in Fig. 4. This graph describes the maximum von Mises stress is about a half of yielding stress set as 1000 GPa while a 0.8 N·m of torque is applied. The actuated rotary movement is about 0.42 degree, which is taken as design value. Moreover, loading capacity of picomotors also needs to be considered. When a 0.8 N·m of torque is produced, reactive force is still under the loading capacity of picomotors.

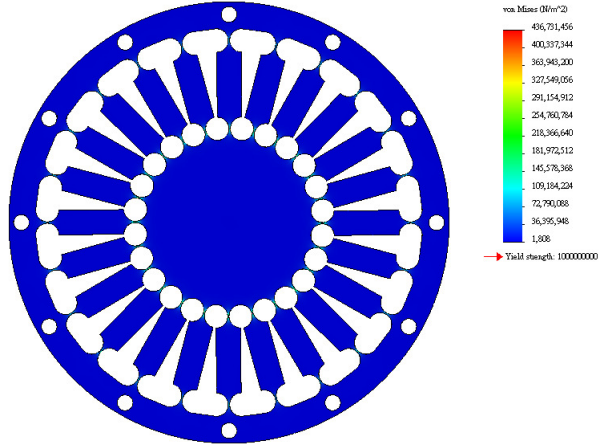


Figure 4: Result of finite-element analysis for rotary weak-link mechanism.

TESTING PROCEDURE AND RESULT

The parallelism between horizontal or vertical pair of blades is hard to measure because of its small opening size. Optical microscope, especially in high magnification, cannot be used due to limitation of depth of field. To overcome the difficulty of verifying the parallelism, the method of single-slit diffraction was used for its convenient observation. Based on the equation of Fraunhofer single-slit:

$$y = \frac{m\lambda D}{a} \quad (1)$$

Symbols y , m , λ , and a from above equation mean displacement from centreline for minimum intensity, order, wavelength of light, distance from slit and screen, and width of slit respectively. Helium-Neon laser with 543 nm of wavelength was used as the source of light in the testing system. Obviously if the displacement from centreline for first minimum intensity which means m equals one is measured, the width of slit can be calculated. Scanning from one side to the other is then made to observe variation of width.

Fig. 5 shows the diffraction pattern observed in the test of parallelism for horizontal slit. After adjusting rotary weak-link structure, the smallest variation of parallelism was about 0.3 μ m less than that of specifications. This result represents not only the testing system is convenient for adjustment of parallelism, but the weak-link mechanism is effective for slightly rotary adjustment.

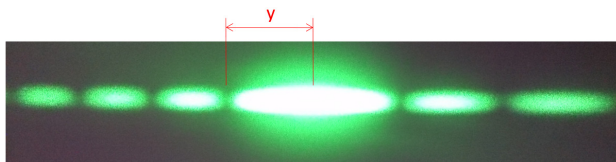


Figure 5: Diffraction pattern observed in the test of parallelism for horizontal slit.

PRECISE TEMPERATURE CONTROLLING SYSTEM

To minimize fluctuation of surrounding temperature for secondary source slits, a precise temperature controlling system is adopted. The system of secondary source slits is planned to be enclosed by a extruded-aluminum frame covered by double layers of plastic curtain and isolated from environment. A compact-type air handling unit (AHU) with coil-type heat exchangers shown in Fig. 6 supplies air with very stable temperature into the enclosed area. According to previous on-site test of this type of AHU in other beamline at TPS, variation of temperature for supplied air in exit port of AHU is within ± 0.02 $^{\circ}\text{C}$. It is also verified that variation of temperature of supplied air in inlet port of enclosed area is within ± 0.03 $^{\circ}\text{C}$.

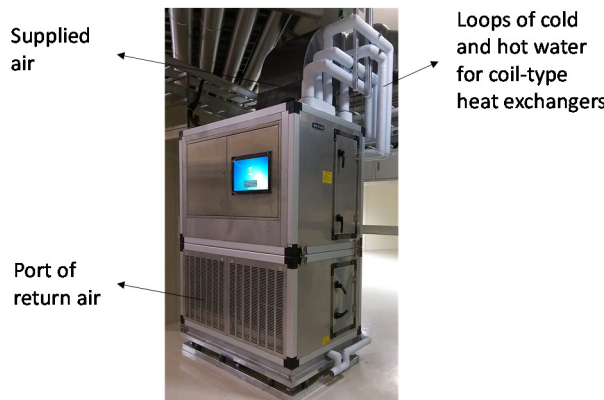


Figure 6: A compact-type air handling unit for precise temperature controlling system.

REFERENCES

[1] D. Shu *et al.*, "Development and applications of a two-dimensional tip-tilting stage system with nanoradian-level positioning resolution", *Nucl. Instr. And Meth. A* , vol. 649, pp. 114-117, 2011.